On the need of fuel modeling for the Harbin Numerical Virtual Reactor (NVR)

ZIMMERMANN Martin A[1]

1. *Senior Advisor Nuclear Safety, CH-5234 Villigen, Switzerland*
   Member of the International Advisory Council to the College of Nuclear Science and Technology, Harbin Engineering University (martin.zimmermann@ensi-rat.ch)

Abstract: The objective of this paper is to propose how research and development of fuel behavior models and the related computational tools should be conducted within the framework of the Virtual Numerical Reactor (NVR) project now on going at the Harbin Engineering University (HEU). The author's proposition ranges from (i) the need of macroscopic fuel modeling, to (ii) the explanation of various phenomena related with the fuel behaviors, to (iii) elements of the thermo-mechanical framework (relevant physical equations) and the related constitutional laws that are necessary, to (iv) the short review of the international trend of related fuel behavior code development and to (v) the way of multi-physics coupling of the fuel pin modeling in the whole NVR. The proposition finally concludes with the importance of building the expertise on fuel behavior modeling for the success of NVR project.

Keyword: numerical virtual reactor; fuel modeling; computation tool of fuel behavior; multi-physics coupling; thermo-mechanical framework

1 Introduction

Beginning of 2017, the second phase of the Numerical Virtual Reactor (NVR) project has started at the College of Nuclear Science and Technology, Harbin Engineering University (HEU). This concept has first been proposed by the Nuclear Power Simulation Research Center at HEU in 2011. It is defined as "science-based, high-fidelity models of neutron transport, thermal-hydraulic, material performance in reactor pressure vessel (RPV) and nuclear steam supply system (NSSS), efficient and robust solver, and high performance computation (HPC) platform" [1] which is able to represent the transient behavior of light-water reactor (LWR) systems with a high degree of fidelity. An important application target has been set for the NVR to become an integral part of the digital design process by providing the simulations necessary for the design evaluation and the corresponding safety assessments. Creating such science-based simulation platform for current and new nuclear reactor systems represents a very ambitious initiative.

In this context, the role of fuel modeling needs to be specified. This paper which grew out of an invited lecture at the 22nd International Workshop on Nuclear Safety and Simulation Technology (IWNSST2017) offers a short review of the modeling for NVR considered necessary for achieving the ambitious goals.

2 Need of macroscopic fuel modeling in the NVR

Multiple barriers and the Defence-in-Depth concept (DiD) as important safety principle were applied from the very beginning of the development of Nuclear Energy. Demonstrating the integrity of the barriers then becomes an important capability necessary for the successful safety demonstration.

For LWRs, the fuel cladding constitutes the first barrier, the reactor pressure vessel (RPV) represents the second barrier, and the containment vessel (CV) is the third barrier. Depending on the frequency of the postulated scenario and as specified by the National Nuclear Regulatory Authority, none, one or two of the barriers could lose integrity.

For the postulated transients with the highest frequency, the first barrier must stay intact. Its demonstration requires detailed modeling of the fuel

Received date: November 20, 2017
(Revised date: January 15, 2018)

pin behavior. This in turn requires power input from the neutronic modeling of the reactor core, ideally resolved to the pin-level, as well as input from core thermal-hydraulics to determine the heat transported away from the cladding surface (cooling) and the heat transfer regime. (See **Fig. 1**.)

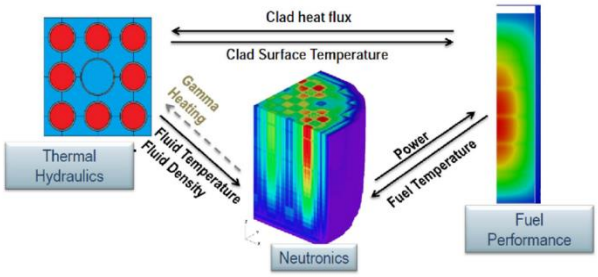

Fig. 1 Multi-physics in the reactor core [1]

A rigorous simulation of the transient behavior of the reactor core forms the basis for the evaluation of the reactor design and its safety performance and allows to demonstrate compliance with the acceptance limits of specified parameters (*e.g.* maximal cladding surface temperature, maximal cladding strain, maximal gap pressure, maximal fuel enthalpy, departure from nuclear boiling [DNB], *etc.*).

3 Short description of the fuel pin

The LWR fuel pin comprises the following elements as you see in **Fig. 2**: A stack of fuel pellets of UO_2, a polycrystalline ceramic material. The fuel pellets are concentrically enclosed by the Zircaloy cladding tube; the cladding tube is closed by the bottom end plug that ensures the proper position in the assembly bottom plate and the top end cap, thereby constituting the first tight barrier around the fuel. The plenum space above the fuel-stack allows for its axial thermal expansion. The fuel-stack hold-down spring in the plenum space keeps the pellets in axial contact. In radial direction, there is an initial gap between the pellet surface and the inner surface of the cladding.

Typical dimensions are ca.400 cm for the fuel-stack length, 35 cm for the plenum, the fuel pin diameter is of the order of 10 mm. The height of the single pellet is ~10mm. The initial radial gap size is between 0.070 mm (PWR) and 0.140 mm (BWR).

The pellet geometry is derived from detailed consideration of thermal and mechanical behavior: The dishing allows for thermal expansion particularly in the pellet center, while the chamfer mitigates the mechanical interactions with the cladding tube when the gap closes. (see **Fig. 3**).

At the begin of life (BOL), the gap is filled with He gas in order to enhance the heat transport from the pellet to the cladding. The fill gas pressure at cold conditions and the size of the gas plenum should be chosen such as to not over-pressurize the fuel pin at hot conditions and with the released fission gases at the end-of-life (EOL).

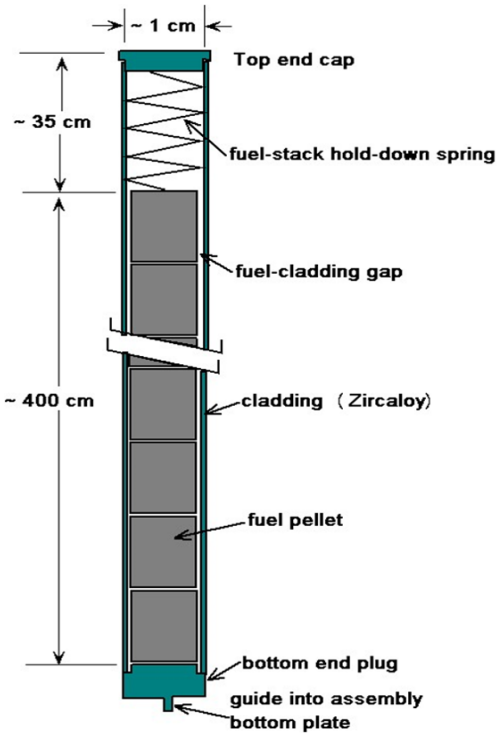

Fig. 2 Outline of LWR fuel pin.

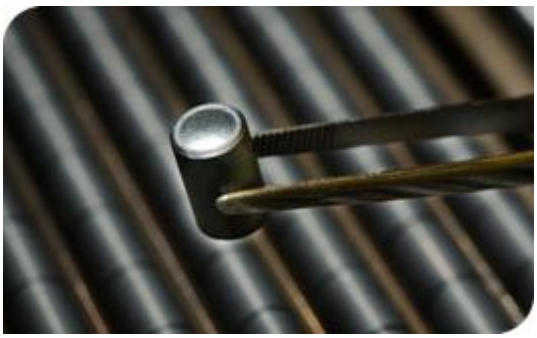

Fig. 3 Nuclear Fuel Pellet, showing central dishing and chamfer at the edge (source: www.us.areva.com, accessed: Nov 4, 2017).

4 Thermo-mechanical framework

If a fuel pin is subjected to temperature transients, then different components may start interacting with each

other, due to the different thermal expansion of the fuel and the cladding material. Since the cladding wall represents the first barrier to the release of radioactivity, all phenomena and processes that ultimately challenge the barrier integrity either during normal operation or during accidental transients must be analyzed. Some of these phenomena occur at BOL (after very short time of operation) while others are the consequence of slower processes which are driven by the fission-induced processes occurring during the fuel pin irradiation in the reactor core.

The determination of the fuel temperature and the stresses in the material form the basis of fuel behavior analysis. Many of the processes occurring in the fuel and the cladding as well as material properties are strongly dependent on temperature.

4.1 Thermal field

The dominant parameter influencing many fuel-behavior phenomena is temperature. The heat generated within the fuel pellets is transported to the pellet surface and across the gap and the cladding to its surface from where it is transported to the coolant. This latter step is governed by the different heat transfer (HT) regimes specific correlations (laws).

Overall, the heat transport is governed by the temperature gradient, as the following equations show (they are valid for isotropic material, for polycrystalline ceramic materials, *e.g.*, UO_2 a good approximation at the macroscopic scale):

$$\rho(\bar{r},T)c_p(\bar{r},T)\frac{\partial T}{\partial t} = \nabla \cdot k(\bar{r},T)\nabla T(\bar{r},t) + q'''(\bar{r}) \quad (1)$$

$\bar{r},T$: location, temperature

$\rho(\bar{r},T)$: density

$c_p(\bar{r},T)$: specific heat

$k(\bar{r},T)$: heat conductance

$q'''(\bar{r})$: volumetric heat generation rate

For steady state, the following Eq. (2) holds:

$$\iiint \nabla \cdot k(\bar{r},T)\nabla T(\bar{r},T) + \iiint q'''(\bar{r},T) = 0$$

$$-\iint \nabla q''(\bar{r},T) + \iiint q'''(\bar{r},T) = 0 \quad (2)$$

where

$q''(\bar{r},T)$: surface heat flux as function of location and temperature

From Eq. (1), it becomes evident that constitutive laws for density, specific heat, heat conductance and the volumetric heat generation rate are necessary.

4.2 Mechanical field

The assessment of the integrity of the cladding requires evaluation of mechanical stresses and resulting strains.

For one-dimensional fuel behavior simulation codes, the following simplifying assumptions are typically assumed:
(1) The fuel pin is assumed to be axisymmetric with no tangential variations.
(2) Although the fuel and cladding move axially (not necessarily at the same rate), cross-sections perpendicular to the z-axis remain plane during deformation (generalized plain strain condition), that is, the rod remains cylindrical.
(3) Elastic constants are often isotropic and constant within a cylindrical ring, although more advanced codes consider the anisotropy.
(4) The total strain can be written as the sum of elastic and non-elastic components.
(5) The inherent time dependence (creep) is handled incrementally (quasi-steady).
(6) Dynamic forces (inertia) are not treated in general.

The mechanical formulas are given for isotropic materials and for axisymmetric geometry which represents a strong simplification. Similar formulas can be developed for three dimensions, for example as seen in [2].

Equation (3) gives the relationship between the radial and tangential stresses, assuming local equilibrium for the radial forces:

$$\frac{d\sigma_r}{dR} + \frac{\sigma_t - \sigma_r}{R} = 0 \quad (3)$$

σ: stress

R: Radius of the deformed geometry

Subscripts:

r: radial direction

t: tangential direction

a: axial direction

Compatibility between strains reduces the following equations by assuming no cracks, hence no discontinuities in displacements:

$$\varepsilon_r = \frac{du}{dR} \;;\; \varepsilon_t = \frac{u}{R} \;;\; \varepsilon_a = C \;\; (const.) \qquad (4)$$

u: radial deformation

$\varepsilon_{r,t,a}$: strain in directions r,t,a,
written as vector in Eq. (4)

The total strain is the sum of elastic and the non-elastic strains:

$$\bar{\varepsilon}^{total} = \bar{\varepsilon}^{elastic} + \sum \bar{\varepsilon}^{nonelastic} \qquad (5)$$

4.2.1 Elastic strains

Elastic strains are reversible for isotropic materials:

$$\varepsilon_r^{elastic} = \frac{1}{E}[\sigma_r - \nu(\sigma_t + \sigma_a)]$$
$$\varepsilon_t^{elastic} = \frac{1}{E}[\sigma_t - \nu(\sigma_a + \sigma_r)] \qquad (6)$$
$$\varepsilon_a^{elastic} = \frac{1}{E}[\sigma_a - \nu(\sigma_r + \sigma_t)]$$

E: elastic Modulus

υ: Poisson ratio

4.2.2 Nonelastic strains

Nonelastic strains consist of many components to be considered in fuel behavior modeling.

(1) Thermal strains:

$\varepsilon_i^t = \alpha(T - T_0)$, i∈$\{r, t, a\}$

α: thermal expansion coefficient, material dependent

(2) Swelling:

$$\varepsilon_{fuel}^s = \frac{1}{2}\left[\left(\frac{\Delta V}{V}\right)_{solid\ FP} + \left(\frac{\Delta V}{V}\right)_{gaseous\ FP} - \left(\frac{\Delta V}{V}\right)_{densification} - \left(\frac{\Delta V}{V}\right)_{hot\ pressing}\right]$$

The swelling due to solid FPs is nearly linearly dependent on burnup, the swelling due to gaseous FPs is due to the formation of fission gas bubbles. Advanced models for fission gas release (FGR) also describe the evolution of the bubble population and can provide this swelling term.

(3) Densification:

The densification term that addresses the re-sintering process early in life of a fuel pin is typically evaluated using empirical correlations, because not all parameters necessary are readily available for a mechanistic model (see also section **5.1.2**).

(4) Plasticity:

Plastic deformations occur instantaneously for stresses beyond the yield point.

For multidimensional stress states, a criterion is necessary to differentiate the amount of elastic and non-elastic stress. This can be done with the help of the van Mises criterion for isotropic materials: The effective stress σ_{eff} should be above the yield stress derived from uni-axial testing (without shear stress):

$$\sigma_{eff} = \frac{1}{\sqrt{2}}[(\sigma_r - \sigma_t)^2 + (\sigma_t - \sigma_a)^2 + (\sigma_a - \sigma_r)^2]^{1/2}$$

Combining σ_{eff} with a flow rule relating the plastic stress components to the incremental plastic strain components, the so-called Prandtl-Reuss rule is obtained: The plastic strain increments are proportional to the stress component deviating from the hydrostatic stress (deviatoric stress).

$$\Delta\varepsilon_i^p = \frac{3\Delta\varepsilon_{eff}^p}{2\sigma_{eff}} S_i \qquad i \in \{r, t, a\}$$

$$S_i = \sigma_i - \sigma_h \;;\; \sigma_h = (\sigma_r + \sigma_t + \sigma_a)/3$$

(5) Creep:

Creep is a time-dependent non-elastic deformation. Three different regimes are considered. Strain-rate equations are available for the different regimes of time-dependent creep, in general relating strain-rate with potentials of σ_{eff} and time in a non-linear manner (*e.g.* Norton-law). Beside the creep induced by mechanical loading, also the neutron-induced creep represents a very relevant phenomenon to be taken into account in fuel behavior modeling.

5 Constitutive laws

Some of the important phenomena that are modelled in typical fuel modeling codes will be briefly described in the following subsections **5.1** and **5.2**.

For more comprehensive and recent reviews, please see [3] and [4] as well as the chapters in these references describing the current knowledge on specific aspects of fuel behavior.

5.1 Fuel related parameters and phenomena

5.1.1 Density

The density of the materials is reduced by their thermal expansion. Furthermore, the initial concentric arrangement of fuel pellet, gas-filled gap

and cladding undergoes important change as the temperature increases (**Fig. 3**), due to the differential thermal expansion of the fuel material (UO_2) and the cladding material (Zircaloy). In consequence, the gas plenum pressure rises due to the reduced space available in the gap and also due to the heating of the fill-gas.

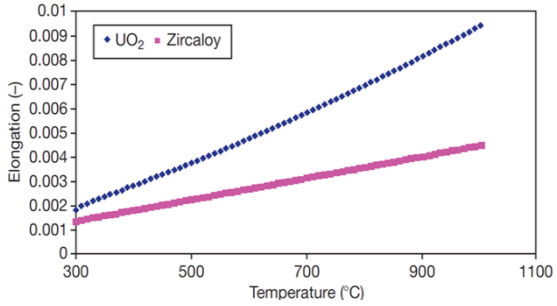

Fig. 3 Elongation of UO_2 fuel and Zircaloy cladding due to thermal expansion as a function of temperature (°C), from [4].

5.1.2 Porosity

The initial porosity of the fuel pellets is first reduced by the so-called re-sintering process at temperature early in life of the fuel (densification), but later starts to grow again due to the swelling caused by the solid fission products that are continuously generated throughout the fuel. This is represented in **(Fig. 4)** that displays the variation in function of burnup of the fuel stack length. Solid fission product swelling represents an additional mechanism reducing the gap size; at high enough burnup, the gap finally closes and contact is established between pellet and cladding, resulting in mechanical (PCMI) and also chemical interaction (PCI).

5.1.3 Specific heat

The specific heat describes the capability to store energy by the fuel materials, strongly influencing its thermal behavior (see Eq. (1)). The vast majority of heat is stored in the fuel pellet. Hence, accurate models for the specific heat of fuel materials are needed. As can be inferred from **Fig. 5**, the specific heat of UO_2 is noticeable smaller than the one for PuO_2 in the range of the operational fuel temperatures of 800 to 1800 K. As PuO_2 is created progressively during the irradiation in LWRs, starting from the pellet periphery, the difference in the respective c_p-values is of relevance.

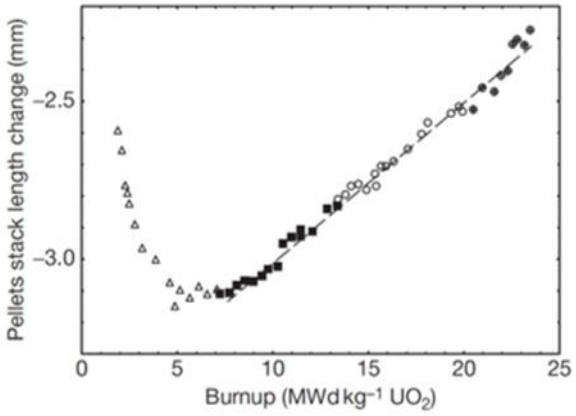

Fig. 4 Change of the fuel pellet stack (mm) as function of burnup [MWd/kg UO2], showing the combined effect of densification and solid fission product swelling [4].

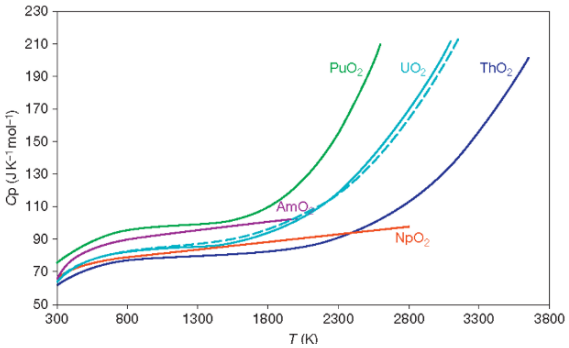

Fig. 5 High-temperature heat capacity of ThO_2, UO_2, PuO_2, NpO_2 and AmO_2 [5]. The dashed line represents the recommendation by Konings [6].

Only relatively few investigations are available on the intrinsic burn-up dependence of c_p. Yet, all the available measurements suggest that within the measurement errors there is no burn-up dependence of c_p.

5.1.4 Heat conductivity

For the heat conductivity, burn-up dependence is established [7], as can be seen in **Fig. 6**. The heat conductivity is reduced with burnup for a given temperature as can be seen in the left backplane at 300 K. For a given level of burn-up, the heat conductivity reduces with increasing temperature. This can most easily be seen on the right back plane for zero burn-up. This diagram shows also that the reduction of the heat conductivity due to irradiation damage tends to disappear at elevated temperatures. For practical application with LWR fuel, a heat conductivity function neglecting irradiation damage yields acceptable fuel temperature results. On one hand, operational fuel temperatures are at a range

where the magnitude of the irradiation induced effect has already become relatively small (ca. 5%) and on the other hand because the heat conductivity diminishes as function of increasing fuel temperature. Many experiments suggest that the effective decrease of the heat conductance during reactor irradiation is due to the following factors:

(i) atomically dispersed fission products (FP), (ii) irradiation and self-irradiation defects, (iii) fission gas and volatile FP dynamically frozen in the fuel during irradiation, and (iv) fission gas precipitation and porosity evolution [6].

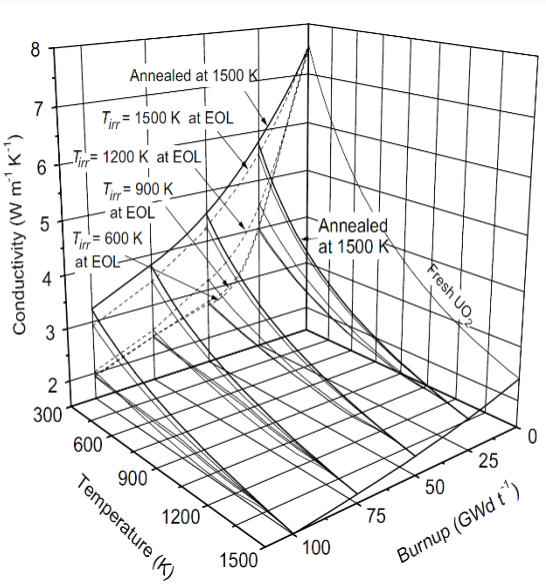

Fig.6 Thermal conductivity of UO2 as a function of temperature, for irradiation temperatures of 600, 900, 1200 and 1500 K, at EOL and after out-of pile annealing up to 1500 K [7].

5.1.5 Volumetric heat generation rate

The volumetric heat generation rate q''' also evolves considerably during the life of a LWR fuel pin due to the gradual build-up of PuO_2 from the periphery towards the pellet center, as can be seen in **Fig. 7**. There are several models available and used in fuel behavior codes describing this effect.

In the case of NVR project, this reactor-physical information should be rather obtained from a detailed core analysis calculation that generates pin-level results.

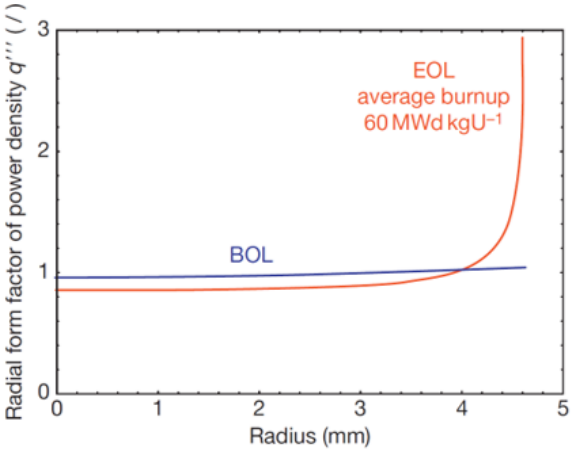

Fig.7 Radial form factor of the power density q''' at BOL and EOL for typical LWR conditions, according to the TURBNP model [8]

With this information, steady-state temperature profiles across a LWR fuel pin can be calculated by assuming a power density of 20 kW/m in the example as shown in **Fig. 8**. The red marks at the left of the diagram show the range of thermocouple measurements taken in a central hole of the IFA-504 test rod irradiated in the Halden reactor in Norway. The two temperature profiles are calculated for a fuel-pin filled with He-gas (representing conditions of a fresh rod) and for a fuel-pin filled with Xe gas that is a gaseous fission product, representing a fuel pin with significant burn-up. Due to the lower heat conductivity of the latter, much higher fuel temperatures result. Note also the significant temperature drop to the left of the zone depicted with "cladding", viz. the gap. This diagram indicates clearly the importance of the gap with respect to heat transfer.

Therefore, an accurate fission gas release model is required for a better prediction of the fuel temperature to capture the heat transfer degrading effect of Xe release to the gap. However, the high importance of gap heat transfer conditions applies only for open gap situations that occur during the first operation cycle. As the gap closes thereafter, the effect of the fission-gas induced heat transfer degradation loses its significance.

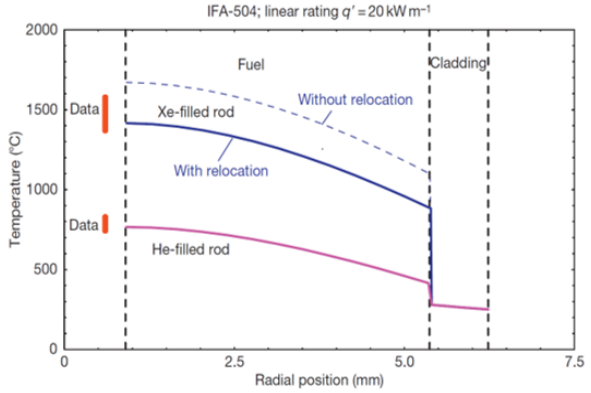

Fig. 8 Radial temperature distribution in a boiling water reactor rod at the beginning of life(BOL). Comparison between the range of experimental results and predictions of the TRANSURANUS code for two different fill gases (He, Xe) [3].

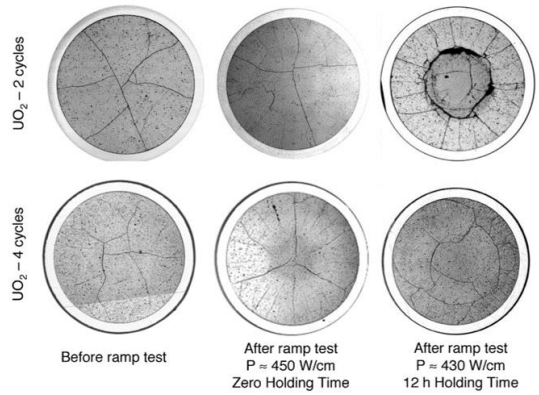

Fig. 9 Cross-sections of UO_2 fuel rodlets (mean burnup ~25 and ~50 GWd/tU) after 2 and 4 cycles irradiation in a commercial PWR (left), after zero holding time power ramps (middle) and after 12 h long power ramps (right) [9]

An additional effect is also shown in **Fig. 8**, where the dashed temperature profile was calculated without considering the so-called fuel-relocation: Thermally induced cracking of the pellet reduces the gap-size with consequent lower fuel temperatures.

5.1.6 Cracking pattern

The evolution of the cracking patterns that is created by stresses due to the thermal gradients can be seen in **Fig. 9**. It reveals burnup dependence as well as dependence on the power history (time at power) [9].

5.1.7 Fission gas release

As already mentioned, fission gas release (FGR) modeling represents another crucial model for any fuel behavior simulation code. Beside purely empirical correlative models as seen in **Fig. 10** in [10], mechanistic models now become standard tools. These models conceptualize fission gas release as a two-step process: The first step addresses the fission gas transport processes within the grains of the polycrystalline UO_2 (intra granular processes), while the second step describes the transport processes along the grain boundaries (inter granular processes). An example of an advanced and very detailed fission gas behavior model is implemented in an operational fuel behavior code [11]. The intra granular processes include generation and dissolution of the fission gas mono-atoms; their diffusion inside fuel grain; coalescence of mono-atoms resulting in formation of bubbles; growth of bubbles due to coalescence and due to the flux of the irradiation-induced point defects from the fuel matrix to the bubbles; and finally, the arrival of the fission gas bubbles at the grain boundary. The inter granular part considers formation of the gas clusters on the grain surface; their evolution resulting in the formation and growth of the closed gas pores; and finally, the conversion of the closed gas pores to the open (vented) pores resulting in the fission gas release into the fuel rod free volume. In addition to the calculation of FGR, the growth of the intra granular bubbles as well as the inter-granular pores determines the corresponding component of the total fuel swelling [11].

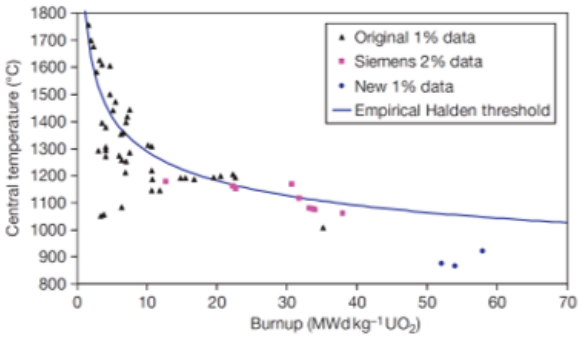

Fig.10 Original Halden (or Vitanza) criterion for the onset of fission gas release and supporting data [10].

5.2 Cladding related parameters and phenomena

As the cladding represents the first barrier, its degradation mechanism is important for the assessment of the cladding integrity during operation and postulated accidents. The mechanical solution will describe the cladding deformations as the function of the applied stress and temperature so that even the prediction of rupture becomes possible. The mechanical solution needs proper materials data, *e.g.* elastic moduli E and G, yield stress, *etc*. The cladding materials undergoes phase transitions at elevated temperatures, with some phases showing non-ductile behavior. The phase transitions depend on temperature and the composition; especially O_2 and H_2 play the important role in this context. Furthermore, H_2 (in supersaturated conditions) may form hydrides that can weaken the mechanical strength of the cladding. Therefore, hydrogen uptake is an important phenomenon.

5.2.1 PCMI

In PCMI situations, at least a 2D mechnical modeling is required for a realistic representation of the cladding deformation, the contact between the deformed fuel pellet and the cladding as well as the resulting stresses deforming the cladding into characteristic ridges (**Fig. 11**). In traditional 1.5D fuel behavior codes, the interaction is represented via an effective friction, but it fails to provide the local details.

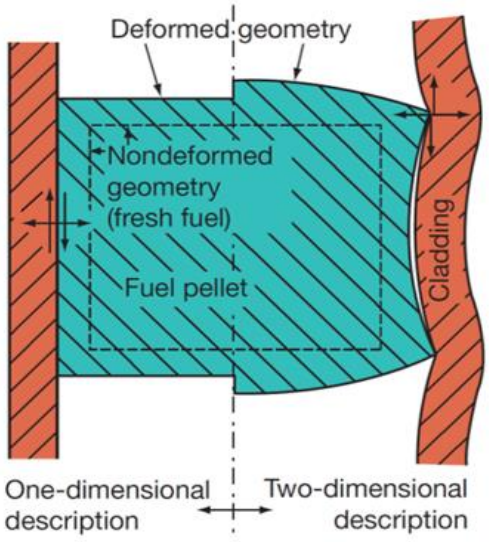

Fig.11 Schematic view of a deformed fuel pellet; comparison between a one-dimensional and a two-dimensional description [4].

5.2.2 Oxidation

Oxidation of the cladding surface during normal operation also weakens the cladding (reduction of the wall thickness, embrittlement), in addition to introducing an additional heat resistivity.

Reducing oxidation is an important driver for the development of new cladding alloys: As the burnup was continuously increased, the oxidation levels reached with Zircaloy-4 became limiting of the fuel operation. As shown in **Fig. 12**, the more advanced alloy M5 (increased concentration of Nb) shows a better oxidation behavior.

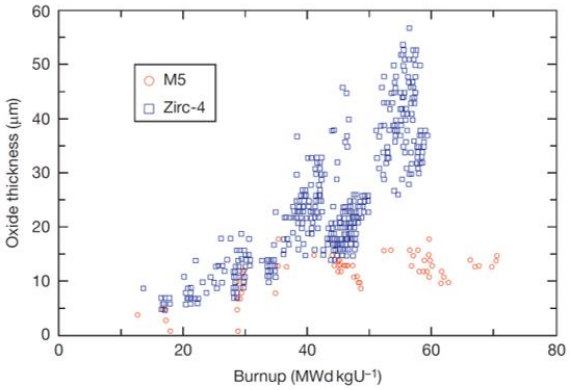

Fig.12 Peak oxide layer thickness as a function of burnup for Zircaloy-4 and Zr1%Nb (M5) [14].

During postulated LOCA accidents, the cladding reaches elevated temperatures and consequently experiences rapid (high-temperature) oxidation. In order to ensure ductility of the cladding throughout the postulated accident, a regulatory acceptance limit is imposed on the maximum oxidation level, together with a maximum concentration of hydrogen in the cladding. Fuel behavior codes that are applied for accident evaluation must include oxidation models to demonstrate compliance with the regulatory limits. Since the existing regulatory limits were derived by using a specific correlation – quite often the Baker-Just correlation - care must be exercised to properly translate the oxidation thicknesses obtained from more modern [best-estimate] correlations such as the Cathcart-Pawel correlation for the demonstration of compliance with the existing regulatory limits.

6 New modelling approaches

Today it is quite evident that the development trend of the fuel behavior codes aims at more detailed modeling. The field equations are solved over 3D grids. The many empirical constitutive laws are partly replaced by new formulations that are informed by the results obtained from advanced methods, such as phase-field modeling, molecular dynamics (MD) or Kinetic Monte Carlo (KMC) to span the whole range of scales of the relevant phenomena. The target is to gradually reduce the empirical laws (correlations) with laws derived from fundamental multi-scale modeling.

Constitutive models (*e.g*. heat conductance) can be informed by results (*e.g.* grain boundary conductance in function of grain boundary coverage with bubbles as a component of the overall heat conductance (*e.g.* [12], [13]) obtained from lower-scale modeling (MD, phase-field modeling). The attempts of adopting more fundamental modeling of phenonmena relevant to fuel behavior are currently an active area of research world-wide. BISON is a respective framework that is actively engaged in adopting the appraoch of implementing models informed from fundamental modeling, see [12], [15]. This example also clearly suggests that the full value of the new constitutive models can only be exploitet by integrating them into an advanced state-of-the-art fuel behavior code, such as *e.g*. BISON.

7 Fuel behavior codes

Quite a number of fuel behavior codes are currently available. Reasonable sources for initial information are available in [4] which offers a list of commonly used codes. A more comprehensive overview is offered in [15] that includes the participants of the FUMEX-III benchmark organised by IAEA. When using this table, the code documentation should be consulted as feasible.

Three additional codes could be mentioned:
(1) ALCYONE 1.4 by CEA [16], a code supporting multidimensional FEM analysis of PWR fuel for base irradiation, ramps and RIA and LOCA accidents.
(2) FRAPTRAN by US NRC [17], a 1.5D FD single-pin fuel behavior code for operational transients and hypothetical accidents. It derives the necessary base irradiation information from FRAPCON that is listed in [4].
(3) SCANAIR by IRSN [18], a 1.5D FEM single-pin fuel behavior code for operational transients and hypothetical accidents.

Obviously, many more codes are around, quite a number of them developed for research purposes and targeted to a specific fuel behavior phenomenon. Among them is DRACCAR [19] that represents a very interesting development: It offers the analysis of a multi-pin assembly with each individual pin capable of ballooning. In this way, flow blockage (coolability) can be assessed in a fully integrated manner.

8 Multi-physics coupling

The many interactions between the thermal and mechanical field are typical for multi-physics coupling. According to [12], one can differentiate between loose and tight coupling.

Loose coupling is characterized by the following considerations:
(i) The distinct physics in a coupled problem are solved individually, keeping the solutions for the other physics fixed.
(ii) After a solution is obtained for an individual physics, it is transferred to other physics that depend on it, and solutions are obtained for those physics.
(iii) If there is no strong two-way feedback between the different physics involved, convergence can be obtained quickly with a minimal number of loose-coupling iterations.

For tight coupling problems, a single system of equations is assembled and solved for the full set of coupled physics. The nonlinear iterations operate on the full system of equations simultaneously, taking into account the interactions between the equations for the coupled physics in each iteration.
The loose-coupling approach is normally adopted for the traditional fuel behavior codes that do not represent contact explicitly. This means that the thermal solution provides input to the mechanical solution only by one-way coupling. In case of thermal contact between solids, *e.g*. gap closure, the

heat conductance depends on the contact pressure; this introduces two-way coupling and makes contact problems computationally challenging [12]. Such a two-way coupling could *e.g*. also be introduced with detailed modeling of fission gas bubbles where the heat conductance across the bubble depends on the bubble size which in turn is influenced by the stresses inside the fuel matrix.

In summary, it is fair to state that the fuel behavior modeling represents one of the best examples of multi-physics two-way coupling in nuclear engineering research.

The modern approach of informing constitutive laws with results and insights obtained from fundamental modeling can be considered as loose multi-scale coupling. Today, this coupling is done mostly outside of the simulation, but efforts are underway to implement such computationally very expensive coupling approaches into (modern) fuel behavior codes on a case by case basis and if access to high-performance computing resources is available.

9 Implications for the Harbin NVR

Considering the goals of the NVR project as introduced in [1], it follows in a straight-forward manner in the view of the author that a strong fuel behavior modeling component must be included into the NVR program. It is as well of great importance to build the expertise on macroscopic fuel behaviour modeling.

The following remarks could be of help in framing the NVR-related R&D work:
(1) Identify a simulation target for fuel behavior modeling within NVR and focus the R&D efforts towards this target. As an example, the capability of a state-of-the art fuel behavior analysis of a RIA-transient could serve as such ambitious target.
(2) Gain experience in operating a operational fuel behavior simulation code and perform the necessary code validation.
(3) Identify the necessary information to be obtained from the other NVR components (viz. neutronics and (core-)thermalhydraulics) and identify and develop the necessary coupling schemes, considering compatibility of the different meshes and loose or tight coupling modes.
(4) Demonstrate the new NVR capability for the already developed validation cases and foremost for the simulation target.

In this way, a modern capability for reactor analysis including fuel modeling could be established and the NVR could truely become one of few operational reactor simulation platforms.

In parallel, it is suggested to further engage in fundamental modeling of well-chosen fuel-behavior phenomena aiming at improving or even replacing the respective purely empirical models, thus reinforcing the efforts of a few similar projects that are already ongoing within the NVR. Initial efforts will likely focus on pristine UO_2, but the real challenge will be to address the impact of the fission products – where applicable – in the fundamental simulations. Adopting this multi-scale approach will give scope for a large number of very interesting research project, *e.g*. PhD-theses.

In the author's view, success of the Harbin NVR can only be reached when maintaining a strong focus on the common over-arching NVR goals.

Nomenclature

BOL: Beginning Of Life
BWR: Boiling Water Reactor
CV: Containment Vessel
DiD: Defence-in-Depth, key safety principle
DNB: Departure from Nucleate Boiling
EOL: End-of-Life
FD: Finite Difference
FGR: Fission Gas Release
FEM: Finite Element Method
FP: Fission Product
HPC: High Performance Computation
HT: Heat Transfer
KMC: Kinetic Monte Carlo
LOCA: Loss of Coolant Accident, design basis accident
LWR: Light Water Reactor (cooling and moderation by water)
MD: Molecular Dynamics
NSSS: Nuclear Steam Supply System

NVR: Numerical Virtual Reactor, a large-size program at the Harbin Engineering University, College of Nuclear Science and Technology.
PCI: Pellet-Clad Interaction
PCMI: Pellet-Clad Mechanical Interaction
PWR: Pressurized Water Reactor
RPV: Reactor Pressure Vessel

References

[1] LEI, L.: Progress on the Numerical Virtual Reactor Project, Harbin: Harbin Engineering University, Presentation to the International Advisory Council on Nuclear Science and Technology, July12, 2017.

[2] BARBER, J.R.: Intermediate Mechanics of Materials, Springer Science+Business Media B.V., 2011.

[3] VAN UFFELEN, P., KONINGS, R.J.M, VITANZA, C., and TULENKO, J.: Analysis of Reactor Fuel Rod Behavior, in CACUCCI, D. (Ed): Handbook of Nuclear Engineering, Vol 3, Reactor Analysis, Springer, 2010, 1520-1627.

[4] VAN UFFELEN, P., and SUZUKI, M.: Oxide Fuel Performance Modeling and Simulations, in KONINGS, R.J.M (Ed in chief): Comprehensive Nuclear Materials, Vol 3, Elsevier, 2012, 535 – 577.

[5] GUENEAU, C., CHARTIER, A., and VAN BRUTZEL, L.: Thermodynamic and Thermophysical Properties of the Actinide Oxides, in KONINGS, R.J.M (Ed in chief): Comprehensive Nuclear Materials, Vol 23, Elsevier, 2012, 21-59.

[6] KONINGS, R. J. M.; BENES, O.; MANARA, D.; SEDMINDUBSKY, D.; GOROKHOV, L.; and IORISH, V. S.: J. Phys. Chem. 2011.

[7] RONCHI, C., SHEINDLIN, M., STAICU, D., and KINOSHITA, M.: Effect of burn-up on the thermal conductivity of uranium dioxide up to 100'000 MWd/t, Journal of Nuclear Materials, 2004, 237:58-76.

[8] LASSMANN, K., WALKER, C.T., and VAN DER LAAR, J.: J. Nucl. Mater., 1998, 255:222-233.

[9] SERCOMBE, J., AUBRUN, I., and NONON, C.: Power ramped cladding stresses and strains in 3D simulations with burnup-dependent pellet–clad friction, Nucl. Eng. Des., 2012, 242:164-181.

[10] VITANZA, C., KOLSTAD, E., and GRAZIANI, C.: Fission gas release from UO_2 pellet at high burnup. In Topical Meeting on Light Water Reactor Fuel Performance, Portland, OR, May 1979; American Nuclear Society: Portland, OR, 1979.

[11] KHVOSTOV, G., MIKITYUK, K., and ZIMMERMANN, M.A.: A model for fission gas release and gaseous swelling of the uranium dioxide fuel coupled with the FALCON code, Nucl. Eng. Des., 211, 241:2983-3007.

[12] HALES, J.D., *et al.*: Advanced multiphysics coupling for LWR fuel performance analysis, Annals of Nuclear Energy, 2015, 84:98-110.

[13] CHEN, T., CHEN, D., SENCER, B.H., and SHAO, L.: Molecular dynamics simulation of grain boundary thermal resistance in UO_2, Journ. Nucl. Mat, 204, 452:364-369.

[14] BOSSIS, P., PECHEUR, D., HANIFI, K., THOMAZET, J., and BLATT, M.: J. ASTM, Int., 2006, 3(1), Paper ID JAI12404.

[15] IAEA: Improvement of Computer Codes Used for Fuel Behaviour Simulation (FUMEX–III), TECDOC-1697, 2013.

[16] MICHEL, B., NONON, C., SERCOMBE, J., MICHEL, F., and MARELLE, V.: Simulation of pellet-cladding interaction with the PLEIADES fuel performance software environment, Nuclear Technology, 2013, 182:124-137.

[17] CUNNINGHAM, M.E., BEYER, C.E., MEDVEDEV, P.G., and BERNA, G.A.: FRAPTRAN: A Computer Code for the Transient Analysis of Oxide Fuel Rods, US NRC, 2001, NUREG/CR-6739, PNNL-13576, Vol. 1-2, Pacific Northwest National Laboratory, Richland, WA.

[18] MOAL, A., GEORGENTHUM, V., and MARCHAND, O.: SCANAIR a transient fuel performance code Part one: General modelling description, Nuclear Engineering and Design, 2014 280:150-171.

[19] BASCOU, S., DE LUZE, O., EDERLI, S., and GUILLARD, G.: Development and validation of the multi-physics DRACCAR code, Annals of Nuclear Engineering, 2015 84:1-18.